Trajectory Design Techniques in the CRTBP for a DS-OTV Mission

Roger Gutierrez-Ramon, *PhD Student, SOKENDAI,* Yuying Liang, *Post-doctoral Fellow, ISAS/JAXA,* Yuto Takei, *JAXA Staff, ISAS/JAXA,* Takanao Saiki, *Researcher, ISAS/JAXA,* Yuichi Tsuda, *Professor, ISAS/JAXA,* Yasuhiro Kawakatsu, *Professor, ISAS/JAXA,*

***Abstract*—The CRTBP (Circular Restricted Three-Body Problem) in its general form is a six dimension problem. In order to design specific trajectories and orbits, intersections between multiple sets of state vectors need to be studied. Although possible, brute-forcing a search of the whole state space of orbits is inefficient and can lead to long computation times. A set of techniques based on parametrization principles as a function of different parameters is presented with the objective of finding intersections between sets of periodic orbit families and natural trajectories derived from them. The results are used as a building block to defining adequate orbits for a DS-OTV (Deep Space Orbit Transfer Vehicle) to be used in future missions, enabling recurring exploration of deep space celestial bodies.**

I. Introduction

The Deep Space Orbit Transfer Vehicle (DS-OTV) has been introduced in the past[1] as part of recent efforts in space exploration to diversify scientific objectives. These novel objectives include missions such as Rosetta[2], OSIRIS-Rex[3], Hayabusa[4] and Hayabusa 2[5], to small celestial bodies. New efforts also take the shape of the creation of novel techniques for space travel, such as solar sails (IKAROS[6], OKEANOS[7]) or continuous low thrust engines (DESTINY$^+$[8]). The DS-OTV concept (Fig. 1) falls in the category of systems that enable repeatable access to space[9], [10], [11], [12], by placing an Orbit Transfer Vehicle (OTV) in a parking orbit in the Earth's vicinity that would be used by successive missions as a refueling station and staging point. The usage of an OTV would allow to bring the launch mass of the mission spacecraft down, increase the availability of launch windows and allow flexibility against delays and launcher vehicles used[13], [14].

R. Gutierrez-Ramon is a PhD Student, Department of Space and Astronautical Science, The Graduate University for Advanced Studies, SOKENDAI, ISAS/JAXA, 252-5210 Kanagawa-ken, Sagamihara-shi, Chuo-ku, Yoshinodai 3-1-1 (e-mail: roger.gutierrez@ac.jaxa.jp).

Y. Liang is a Post-doctoral Fellow, Department of Solar System Science, ISAS/JAXA, 252-5210 Kanagawa-ken, Sagamihara-shi, Chuo-ku, Yoshinodai 3-1-1

Y. Takei is a Hayabusa 2 Project Member at ISAS/JAXA, 252-5210 Kanagawa-ken, Sagamihara-shi, Chuo-ku, Yoshinodai 3-1-3.

T. Saiki is a Researcher at the Department of Space and Astronautical Science, ISAS/JAXA, 252-5210 Kanagawa-ken, Sagamihara-shi, Chuo-ku, Yoshinodai 3-1-3.

Y. Tsuda is a Professor at the Department of Space and Astronautical Science, ISAS/JAXA, 252-5210 Kanagawa-ken, Sagamihara-shi, Chuo-ku, Yoshinodai 3-1-3.

Y. Kawakatsu is a Professor at the Department of Space and Astronautical Science, ISAS/JAXA, 252-5210 Kanagawa-ken, Sagamihara-shi, Chuo-ku, Yoshinodai 3-1-3.

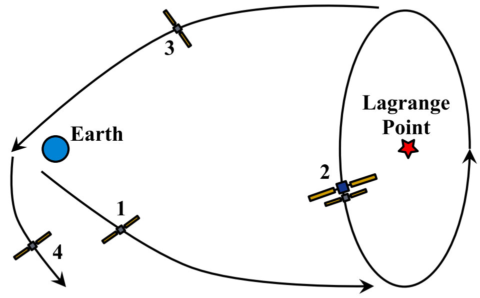

Fig. 1: DS-OTV architecture. 1) The spacecraft transfers to the DS-OTV parking orbit. 2) It docks with the DS-OTV to re-fuel. 3) It undocks and leaves the parking orbit. 4) After an Earth Swing-by, the spacecraft starts its journey to the objective.

The feasibility of such an architecture depends, among many factors, on the orbital placement of the OTV and its ease of access from the Earth. Orbits in the vicinity of the $L_{1,2}$ Lagrange Points (which have been studied in the past[16], [17]) are interesting, as well as the transfers between them, as the combinations of these orbits can be advantageously used during the time of OTV and mission spacecraft combined use. We previously studied these transfers, but restricted ourselves to the simplest case, where both orbits intersect at the symmetry axis, once per orbital period.[15] While this case is the most efficient one fuel-wise, it comes with strong constraints in the operations department. Therefore, finding orbital pair crossings that occur multiple times per orbital period seems the next step in order to alleviate some of these constraints.

In this work, we introduce a novel algorithm that leverages parametrization and fitting techniques and is designed to find combinations of orbits with multiple crossings for each orbital period. We study a subset of candidate periodic orbit families for the OTV's parking orbits by applying this algorithm with the focus on the characterization of the transfers between them with regards to availability, fuel usage and maneuver time. The two-step algorithm designed separates the initial localization of the crossings' area and the refinement of the solution. In this way, the more computationally intensive calculations are done over a smaller set of possible solutions, and the overall process is faster. The results are obtained and analyzed to find the general structure concerning the full orbital families, and for such an objective, appropriate nomenclature and concepts are introduced and explained.

II. Dynamical Model and Orbits Generation

A. The Circular Restricted Three-Body Problem

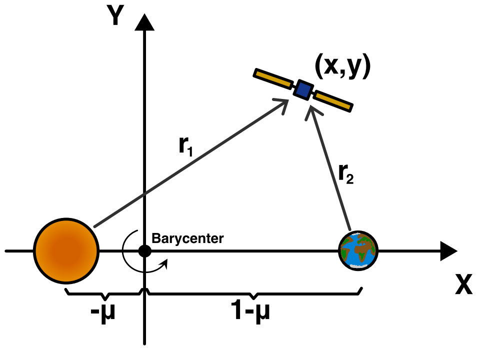

Fig. 2: The Circular Restricted Three-Body Problem (CRTBP).

The dynamical model used in this research is the Circular Restricted Three-Body Problem (CRTBP), where a massless spacecraft moves in the gravity field of two massive bodies, which revolve around their barycentre in a circular motion. In this Sun-Earth system, the total mass of the Sun and Earth is normalized to 1, the distance between the Sun and the Earth is normalized to 1, and the period of the Earth's orbit is normalized to 2π. We define a rotating frame with the origin at the barycenter of the system, the x-axis coincides with the Sun-Earth line and is positive in the Sun-Earth direction, the y is positive in the direction of the Earth's velocity, and the z-axis completes the right-handed coordinate system. By defining the rotation period of the system equal to the period of the Earth, both bodies remain on the x-axis. The mass ratio of the system is defined as $\mu = \frac{m_{\text{Earth}}}{m_{\text{Sun}}+m_{\text{Earth}}}$, so the coordinates of the Sun are $(-\mu, 0)$, and the coordinates of the Earth $(1-\mu, 0)$, as shown in Fig. 2. With the spacecraft's coordinates (x, y, z), the equations of motion are written as

$$\begin{aligned} \ddot{x} - 2\dot{y} &= \Omega_x \,, \\ \ddot{y} + 2\dot{x} &= \Omega_y \,, \\ \ddot{z} &= \Omega_z \,, \end{aligned} \tag{1}$$

where

$$\Omega(x, y, z) = \frac{1}{2}\left(x^2 + y^2\right) + \frac{1-\mu}{r_1} + \frac{\mu}{r_2} + \frac{\mu(1-\mu)}{2} \tag{2}$$

The subscripts of Ω in Eq. (1) denote the partial derivatives with respect to the coordinates of the spacecraft. In Eq. (2), r_1 and r_2 denote the distances from the spacecraft to the Sun and Earth respectively as

$$\begin{aligned} r_1 &= \sqrt{(\mu + x)^2 + y^2 + z^2} \,, \\ r_2 &= \sqrt{(1 - \mu - x)^2 + y^2 + z^2} \,. \end{aligned} \tag{3}$$

A first integral of motion, the Jacobi Integral, and its constant of integration, the Jacobi Constant, are defined as

$$C = x^2 + y^2 + \frac{2\,(1-\mu)}{r_1} + \frac{2\mu}{r_2} + \mu(1-\mu) - \dot{x}^2 - \dot{y}^2 - \dot{z}^2 \,. \tag{4}$$

The CRTBP has five equilibrium points (also known as Lagrange or Libration points). Table I lists the parameters for the Sun-Earth used in this research, as well as the positions of these Lagrange points.

TABLE I: Parameters of the Sun-Earth System used in this research. Retrieved from SPICE.[18], [19]

Parameter	Value
Mass ratio	$3.003480594 \cdot 10^{-6}$
Characteristic Length	149597870.7 km
Characteristic Time	365.25635 days
Characteristic Velocity	29.7847 km/s
L_1 admin. coordinates	$(0.990026594, 0)$
L_2 admin. coordinates	$(1.010034116, 0)$
L_3 admin. coordinates	$(1.000001251, 0)$
L_4 admin. coordinates	$(0.499996997, 0.866025404)$
L_5 admin. coordinates	$(0.499996997, -0.866025404)$

B. Periodic Orbits Generation

In this research, a differential correction (single shooting algorithm) is used to find periodic orbits. The search for a periodic orbit is simplified by applying the Periodicity Theorem of Roy and Ovenden (1955).[20] The corrector algorithm is based on a first-order Taylor series expansion of the periodicity conditions. We use the State Transition Matrix (STM $\mathbf{\Phi}$), a linearization method that maps changes to the initial conditions to changes in the state vector at some short time t later. The algorithm comes from [17] and [21], and will be omitted for brevity's sake. See [15] for a detailed explanation.

We generate periodic orbits in the Earth's vicinity and classify them in families. Our main focus is to group orbits that share common interesting properties, so the search is not exhaustive and the classification given in this paper overlaps parts of families described in literature. Due to this, we label the families descriptively and provide a short description. See [15] for the full description, but in general terms, we restrict further research to the Laypunov and Low Prograde Orbit families (shown in Fig. 3) due to the following reasons:

- Both families overlap in the configuration space.
- Both families have a region with very similar levels of the Jacobi Constant.
- A portion of the Low Prograde family has low Earth altitudes, while on the other extreme they get very close to the configuration space of the Lyapunov family.

These reasons lead us to believe that a combination of orbits from these families can be successfully used in the DS-OTV context, more specifically, due to the possibilities of transfers between them. For brevity's sake, only the results for the L_1 Lagrange Point orbital families are shown in the manuscript, but equivalent results are found in the L_2 orbits of families.

III. Single Orbit Dual Insertion Transfers Between Low Prograde and Lyapunov Orbits

The transferring/docking maneuver between orbits is critical to the success of the mission. For Single Orbit Transfers, only one maneuver is possible at each orbital period, which might constrain the mission design too much, making the mission timeline excessively long. Finding the correct procedure is critical. A Single Orbit Dual Insertion scheme, where the orbits intersect twice each orbital period might work, as the time between crossings is shorter than the full orbital period, but might be long enough for the routine proximity operations.

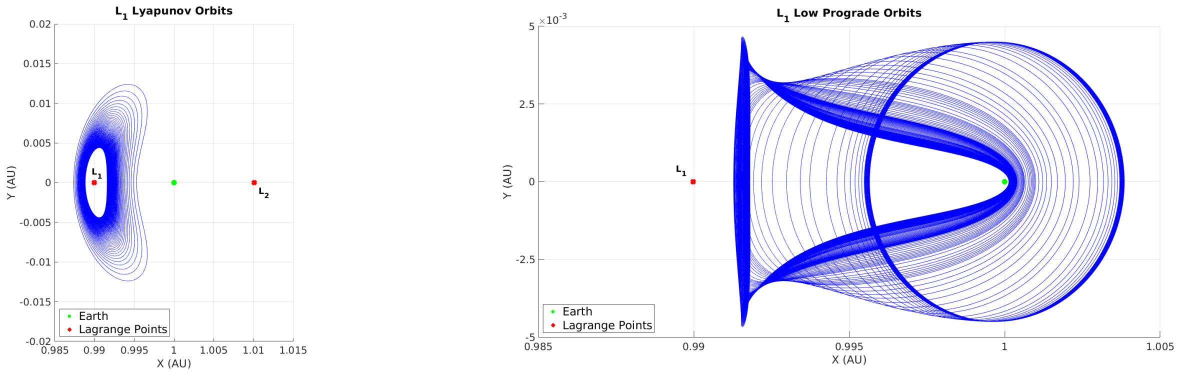

(a) L_1 Lyapunov Orbits (b) L_1 Low Prograde Orbits

Fig. 3: Planar Periodic Orbit families in the Earth's vicinity used in this research. Earth size not to scale.

TABLE II: Parameters of the SODI scheme in Fig. 4.

Parameter	Value
Parking Orbit Period	176 days
Insertion to Parking Orbit Δv	158.4 m/s
Escape from Parking Orbit Δv	158.1 m/s
Total manoeuver Δv	316.5 m/s
Max docking time	40 days

Figure 4 shows a handpicked example of such a maneuver, with Table II summarizing its properties. However, finding these crossings between the full families of orbits carries high computation costs due to them not being in easily definable planes. This is compounded by the high number of orbits that need to be studied if general results want to be obtained. We created a new algorithm to aid in the search and characterization of these crossings.

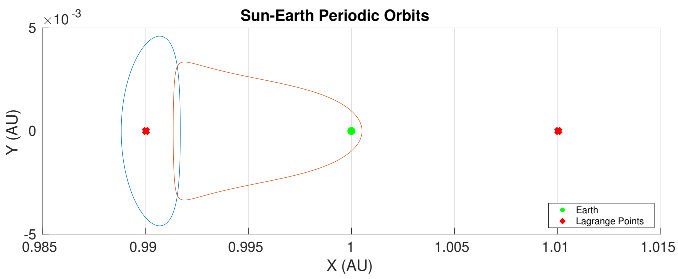

Fig. 4: Single Orbit Dual Insertion (SODI) scheme.

IV. Parametrization-Fit Crossings Algorithm

To search for combinations of Low Prograde and Lyapunov Orbits with multiple crossings, we developed the Parametrization-Fit (Param-Fit) Crossings algorithm. This algorithm circumvents the need to restrict first the phase space location of the crossings (i.e. creating a Poincare Section in the desired crossing search space), as in this case we don't know beforehand where the intersections are located. We use a parametrization and curve fitting technique to simplify the search. The Param-Fit Crossings algorithm consists of the parametrization of the family of orbits, and then a two-step search of the crossings. Fig. 5 summarizes the algorithm, while the following subsections go into detail.

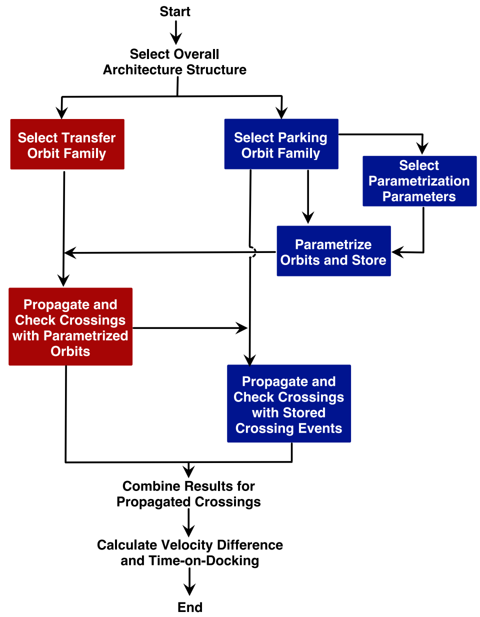

Fig. 5: Flow Chart summary of the Single Orbit Dual Insertion (SODI) Finding Algorithm.

A. *Orbit Parametrization and Analytical Expression Fit*

We parametrize the Lyapunov Orbit family by using polar coordinates. We use the Lagrange Point as center, and parametrize in terms of the angle from the positive x-axis in the counter-clockwise direction (Fig. 6, left).

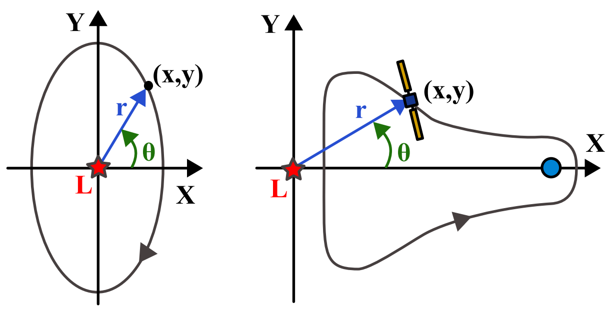

Fig. 6: Lyapunov (left)) and Low Prograde (right) Orbits, parametrized with angle θ.

Since the overlap in the families is happening in the inner section of the Lyapunov Orbit (the region between the Lagrange Point and the Earth), we can parametrize only that part of the orbit. We obtain a 1-to-1 map from polar angle to radius (Fig. 7a). We fit an analytical expression to the curve created by the parametrized coordinates. The best results were obtained by approximating the orbits with a trigonometric Fourier Series, which takes the form

$$r = a_0 + \sum_{i=1}^{n} a_i \cos(iw\theta) + b_i \sin(iw\theta) \ . \tag{5}$$

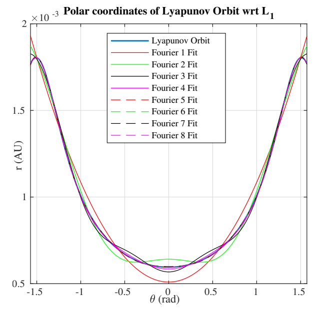

(a) Polar coordinates and Fourier (1-8 orders) Fits for a parametrized Lyapunov Orbit with respect to the L point.

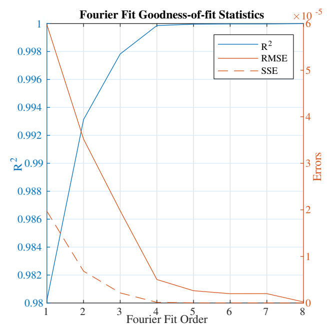

(b) Fourier Fit Goodness-of-fit with respect to the fit order. Statistics for the orbit in Fig. 7a

Fig. 7: Parametrized Lyapunov Orbit Fourier 1-8 Fits (Fig. 7a) and their respective statistics in Fig. 7b.

Fourier series orders 1-8 were tested, and the error obtained is shown in Fig. 7b. Since the evaluation time between different orders Fourier series is negligible, we decided a Fourier 8 fit, as it gave the best goodness-of-fit statistics and less accumulated error. The resulting expression for each orbit consists of a constant term and 16 trigonometric terms.

B. Param-Fit Crossings Algorithm Fist Step

The first step uses the propagated Low Prograde Orbits and searches crossings with the parametrized expressions of the Lyapunov Orbits. For each propagated point, the state vector is converted to polar coordinates (Fig. 6, right). At each time step the crossing check is executed with each parametrized Lyapunov Orbit. The crossing check is

$$r_{\text{Param LO}}(\theta_{\text{LPO},t}) - r_{\text{LPO}_i,t} = 0 \ , \tag{6}$$

where r and θ are the polar coordinates of a propagated point of orbit i at time t for the Low Prograde Orbit, and the evaluation of the analytical expression obtained from parametrizing the Lyapunov Orbits.

C. Param-Fit Crossings Algorithm Second Step

The second step of the algorithm takes as input the results of the first step and refines them. It searches for the intersections between the CRTBP-propagated Lyapunov Orbits and the stored crossings, and saves the data for the Lyapunov Orbit. With this refining step, we obtain a very good approximation of crossing events between the two propagated trajectories.

The second step check takes the form

$$r_{\text{stored LPO crossings}_i} - r_{\text{LO}_i,t} = 0 \ , \tag{7}$$

with r being the distance in polar coordinates of a propagated point of orbit i at time t for the Lyapunov Orbit, and the stored results of the first check for the Low Prograde Orbit. Due to numerical particularities, however, the condition is impossible to meet. By definition the distance (in absolute value) does not exist as a negative (see Fig. 8, left). To solve this, we search for a minimum of the distance during the propagation by evaluating the derivative of the expression to zero (Fig. 8, right), and we verify that we find a minima, while deleting the false-positive maxima points.

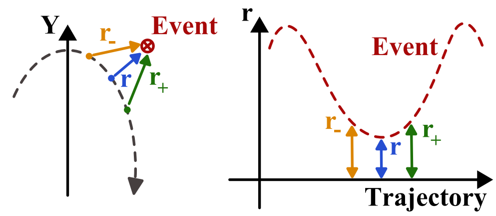

Fig. 8: Crossing event check (left) and event distance minimum search graph (right).

D. Results Database and new SODI Concepts

After running a cleaning algorithm to verify the integrity of the results, the Param-Fit Crossings Algorithm stores the results in a database. The database structure allows for the search of different combinations of crossings to form maneuvers, as well as the creation of new concepts to evaluate the crossing possibilities.

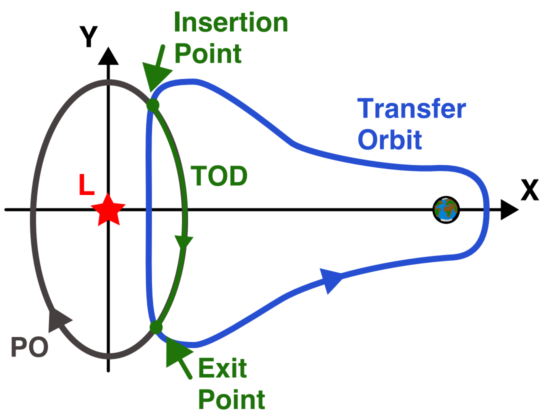

Fig. 9: A Single Orbit Dual Insertion maneuver, with the Time-on-Docking (TOD) marked.

A continuation we will define the quantitative properties to be used in the analysis and comparison. With Fig. 9 showing a basic SIDO scheme maneuver, where a Lyapunov and a Low Prograde Orbit have symmetric crossing points with respect to the x-axis, we define the following:

- Δv - Difference in instantaneous velocity needed to change a spacecraft's state vector.
- Maneuver - The Δv between the state vectors at the crossing points.

- Time-on-Docking (TOD) - The time elapsed between two crossings in the Parking Orbit (Lyapunov in this case).
- Full Maneuver - Each of the two crossings between the Transfer Orbit and the Parking Orbit.

V. Single Orbit Dual Insertion Transfers Results

The results obtained by the application of the Param-Fit Crossings Algorithm to the full L_1 Lyapunov and Low Prograde Orbit families are presented in Fig. 10. The TOD in days is on the x-axis and the full maneuver Δv absolute value in km/s on the y-axis. We see that there are combinations with TODs in the whole interval $0 \leq TOD \leq 53$ days. Moreover, the whole interval is available for low Δv values, less than 0.2 km/s. The most interesting combinations are at the lower part of the graph, showing that for similar amounts of Δv, the entire range of TOD solutions is available. Highlighted are some example combinations to get a more visual intuition. Figure 10a to Fig. 10d show combinations in the lower Δv region, with TODs of 2, 16, 31 and 48 days respectively, while having a Δv of less than 0.2 km/s. All the orbits in these combinations have approximately the same sizes, which puts the crossing points in regions where the velocity vectors have the same overall direction (and thus lower Δv differences). The higher Δv combinations happen when the Lyapunov Orbits become considerably larger than the Low Prograde Orbits. In these cases, the Lyapunov Orbits' trajectories in the regions where the crossings occur have higher velocity values, which coupled with crossing points where the velocity vectors are almost perpendicular, make the full maneuver Δv considerably higher. The overall shape of the figure shows that the higher the Δv of the maneuvers, the less availability of TOD possibilities. An explanation for this phenomenon is that starting at a certain size of the Lyapunov Orbit, most of the crossings with the Low Prograde Orbits occur at roughly the same physical space. Combining this with the increase of size (and velocity) of the Lyapunov Orbits, it means that the TODs availability is reduced (while the Δv keeps increasing).

VI. Conclusion

In this paper we showcased a novel algorithm to find intersections/connecting trajectories in the CRTBP. This algorithm can be used to aid in the preliminary research for a new DS-OTV Mission. From previous research, we selected candidate periodic orbits in the vicinity of the Earth that show potential to be used as parking/transfer orbits in the DS-OTV context. A usage of such orbit combinations could include the transfer from launch to the vicinity of the Lagrange Point, insertion to the parking orbit, docking and refueling, and then immediately exit again to the same transfer orbit, keeping the time spent in stand-by low. The novel Param-Fit Crossings Algorithm was then applied to the subset of Lyapunov and Low Prograde Orbits to find direct transfer maneuvers between them by identifying intersection points. The algorithm introduced uses a combination of parametrization and curve fitting techniques, as well as exploiting the symmetries of the CRTBP, to separate the problem into an effective two-step algorithm to find the orbital crossings. We described the algorithm in detail, and introduced the new concepts used to evaluate the adequacy and usefulness of the crossings found. We found that orbits with combinations of low fuel usage and a wide array of TOD possibilities exist for these families of orbits, which can be useful for the future of the DS-OTV concept.

In addition, an algorithm that combines the usage of parametrization and fitting techniques, such as the one introduced here, can be used for future studies in the CRTBP concerned with finding intersections or connecting trajectories. Such future studies are already planned, and will complement the results presented here by evaluating the phasing and rendezvous possibilities of two spacecraft orbiting the same orbit.

Acknowledgment

The Ministry of Education, Culture, Sports, Science and Technology (MEXT) of the Japanese government supported Roger Gutierrez-Ramon under its program of scholarships for graduate school students.

Yuying Liang acknowledges the financial support of International Research Fellow of Japan Society for the Promotion of Science (Postdoctoral Fellowships for Research in Japan (Standard)).

References

[1] Y. Kawakatsu, “Concept study on deep space orbit transfer vehicle,” *Acta Astronautica*, vol. 61, no. 11-12, pp. 1019–1028, Dec. 2007. [Online]. Available: https://www.sciencedirect.com/science/article/pii/S0094576507001300

[2] K.-H. Glassmeier, H. Boehnhardt, D. Koschny, E. Kührt, and I. Richter, “The Rosetta Mission: Flying Towards the Origin of the Solar System,” *Space Science Reviews*, vol. 128, no. 1, pp. 1–21, 2007. [Online]. Available: http://dx.doi.org/10.1007/s11214-006-9140-8

[3] E. Beshore, B. Sutter, R. Mink, D. Lauretta, M. Moreau, W. Boynton, J. Dworkin, D. Everett, C. Shinohara, and J. Gal-Edd, “The OSIRIS-REx asteroid sample return mission,” in *2015 IEEE Aerospace Conference*. IEEE, Mar. 2015.

[4] J. Kawaguchi, A. Fujiwara, and T. Uesugi, “Hayabusa — its technology and science accomplishment summary and Hayabusa-2,” *Acta Astronautica*, vol. 62, no. 10–11, pp. 639–647, 2008. [Online]. Available: http://www.sciencedirect.com/science/article/pii/S0094576508000441

[5] Y. Tsuda, M. Yoshikawa, M. Abe, H. Minamino, and S. Nakazawa, “System design of the Hayabusa 2—Asteroid sample return mission to 1999 JU3,” *Acta Astronautica*, vol. 91, pp. 356–362, 2013. [Online]. Available: http://www.sciencedirect.com/science/article/pii/S009457651300218X

[6] Y. Tsuda, O. Mori, R. Funase, H. Sawada, T. Yamamoto, T. Saiki, T. Endo, K. Yonekura, H. Hoshino, and J. Kawaguchi, “Achievement of IKAROS — japanese deep space solar sail demonstration mission,” *Acta Astronautica*, vol. 82, no. 2, pp. 183–188, Feb. 2013.

[7] O. Mori, J. Matsumoto, T. Chujo, M. Matsushita, H. Kato, T. Saiki, Y. Tsuda, J. Kawaguchi, F. Terui, Y. Mimasu, G. Ono, N. Ogawa, Y. Takao, Y. Kubo, K. Ohashi, A. K. Sugihara, T. Okada, T. Iwata, and H. Yano, “Solar power sail mission of OKEANOS,” *Astrodynamics*, Oct. 2019.

[8] K. Nishiyama, Y. Kawakatsu, H. Toyota, R. Funase, and T. Arai, “DESTINY$^+$: A Mission Proposal for Technology Demonstration and Exploration of Asteroid 3200 Phaethon,” in *31st International Symposium on Space Technology and Science*, 2017, pp. 1–5.

[9] M. Mammarella, P. M. Vernicari, C. A. Paissoni, and N. Viola, “How the lunar space tug can support the cislunar station,” *Acta Astronautica*, vol. 154, pp. 181–194, Jan. 2019.

[10] M. Matsumoto, “Deep space transportation system using the sun-earth l2 point,” in *20th International Symposium on Space Flight Dynamics*, Sept. 2007.

[11] H. Kalita, M. Donayre, V. Padilla, A. Riley, J. Samitas, B. Burnett, E. Asphaug, M. Robinson, and J. Thangavelautham, “Gnc challenges and opportunities of cubesat science missions deployed from the lunar gateway,” *Advances in the Astronautical Sciences*, Jan. 2019.

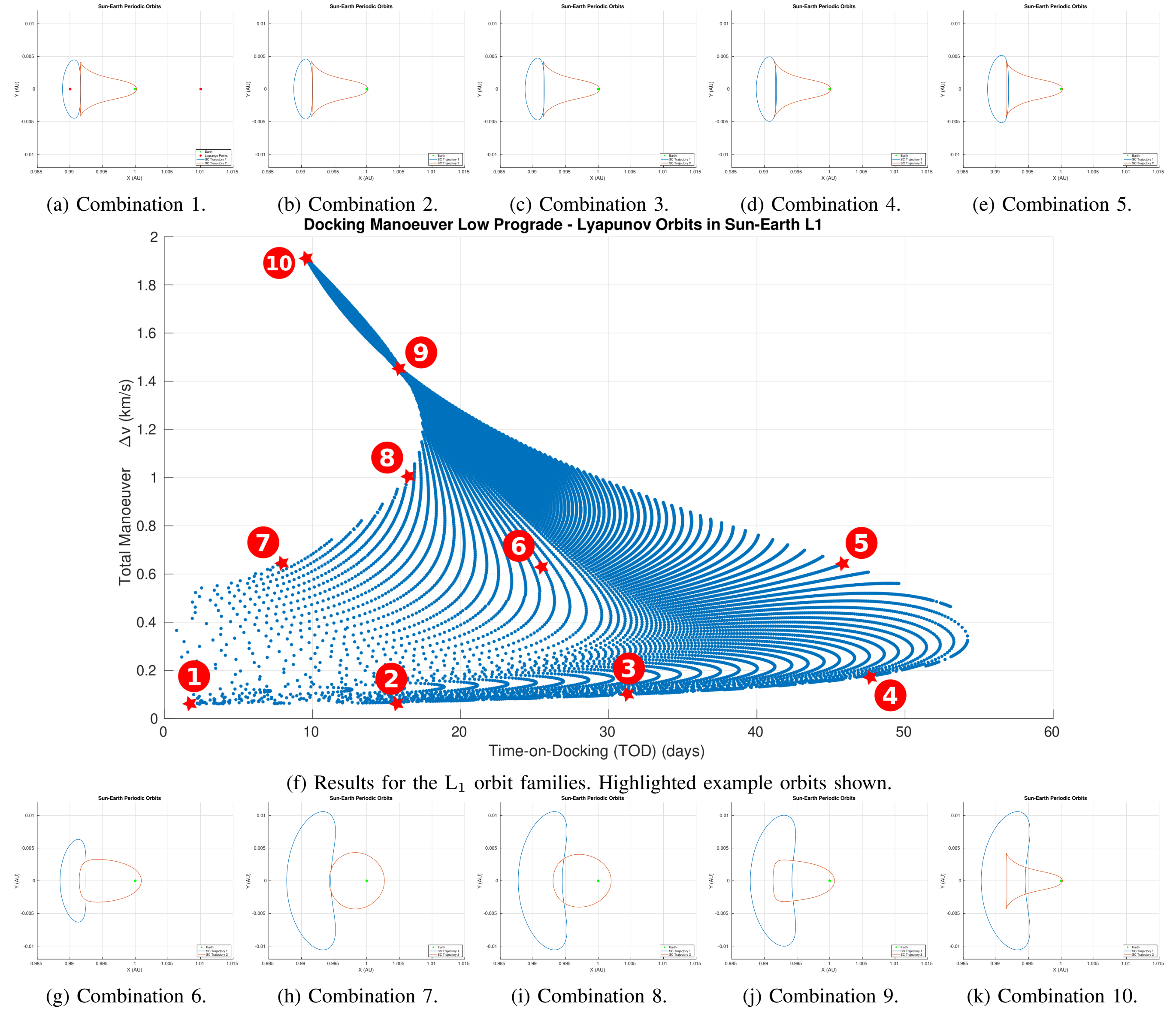

(a) Combination 1. (b) Combination 2. (c) Combination 3. (d) Combination 4. (e) Combination 5.

(f) Results for the L_1 orbit families. Highlighted example orbits shown.

(g) Combination 6. (h) Combination 7. (i) Combination 8. (j) Combination 9. (k) Combination 10.

Fig. 10: SODI Maneuver Δv (insertion to and exit from Lyapunov Orbit) vs TOD (Time-on-Docking, time spent in the Lyapunov Orbit between the two maneuvers). Highlighted are some selected example orbits.

[12] Y. Liang, M. Xu, K. Peng, and S. Xu, "A cislunar in-orbit infrastructure based on p:q resonant cycler orbits," *Acta Astronautica*, vol. 170, pp. 539–551, 2020. [Online]. Available: http://www.sciencedirect.com/science/article/pii/S0094576520300916

[13] S. Mori, A. Saito, M. Arita, M. Okada, A. Sato, M. Niitsu, and T. Nara, "H3 launch vehicle development concept of operations," in *14th International Conference on Space Operations*. American Institute of Aeronautics and Astronautics, May 2016, p. 2531.

[14] R. Gutierrez-Ramon, Y. Tsuda, T. Saiki, Y. Takei, Y. Mimasu, Y. Maru, S. Nonaka, and S. Tokudome, "Concept and feasibility of a deep space orbit transfer vehicle," in *UKAREN 64 Space Science and Technology Association Conference*, no. OS33, Oct. 2020.

[15] R. Gutierrez-Ramon, Y. Liang, and Y. Tsuda, "Design of a deep space orbit transfer vehicle (ds-otv) architecture," in *2020 AAS/AIAA Astrodynamics Specialist Conference*, no. AAS 20-532, American Astronautical Society. American Astronautical Society, July 2020.

[16] K. C. Howell, "Three-Dimensional Periodic Halo Orbits," *Celestial Mechanics*, vol. 32, no. 1, p. 53, Jan. 1984.

[17] W. S. Koon, M. W. Lo, J. E. Marsden, and S. D. Ross, *Dynamical Systems, the Three-Body Problem and Space Mission Design*. Marsden Books, 2011.

[18] C. Acton, N. Bachman, B. Semenov, and E. Wright, "A look towards the future in the handling of space science mission geometry," *Planetary and Space Science*, vol. 150, pp. 9–12, 2018, enabling Open and Interoperable Access to Planetary Science and Heliophysics Databases and Tools. [Online]. Available: https://www.sciencedirect.com/science/article/pii/S0032063316303129

[19] W. M. Folkner, J. G. Williams, D. H. Boggs, R. S. Park, and P. Kuchynka, "The Planetary and Lunar Ephemerides DE430 and DE431," National Aeronautics and Space Administration, The Interplanetary Network Progress Report Volume 42-196, Feb. 2014. [Online]. Available: https://ipnpr.jpl.nasa.gov/progress_report/42-196/196C.pdf

[20] A. E. Roy and M. W. Ovenden, "On the occurrence of commensurable mean motions in the solar system. The mirror theorem," *Monthly Notices of the Royal Astronomical Society*, vol. 115, p. 296, Jan. 1955.

[21] I. A. Robin and V. V. Markellos, "Numerical determination of three-dimensional periodic orbits generated from vertical self-resonant satellite orbits," *Celestial mechanics*, vol. 21, no. 4, pp. 395–434, May 1980. [Online]. Available: https://doi.org/10.1007/BF01231276